Electron-spin polarization of photoions produced through photoionization from the laser-excited triplet state of Sr

Nobuaki Yonekura
Department of Chemistry, Biology, and Marine Sciences, University of the Ryukyus, Okinawa 903-0213, Japan

Takashi Nakajima[a)]
Institute of Advanced Energy, Kyoto University, Gokasho, Uji, Kyoto 611-0011, Japan

Yukari Matsuo, Tohru Kobayashi, and Yoshimitsu Fukuyama
The Institute of Physical and Chemical Research (RIKEN) 2-1 Hirosawa, Wako, Saitama 351-0198, Japan

(Received 2 September 2003; accepted 31 October 2003)

We report the detailed experimental study on the production of electron-spin-polarized Sr^+ ions through one-photon resonant two-photon ionization via laser-excited $5s5p\,^3P_1$ ($M_J=+1$) of Sr atoms produced by laser-ablation. We have experimentally confirmed that the use of laser-ablation for the production of Sr atoms prior to photoionization does not affect the electron-spin polarization. We have found that the degree of electron-spin polarization is $64\pm9\%$, which is in good agreement with our recent theoretical prediction. As we discuss in detail, we infer, from a simple analysis, that photoelectrons, being the counterpart of electron-spin-polarized Sr^+ ions, have *approximately* the same degree of electron-spin polarization. Our experimental results demonstrate that the combined use of laser-ablation technique and pulsed lasers for photoionization would be a compact and effective way to realize a pulsed source for spin-polarized ions and electrons for the studies of various spin-dependent dynamics in chemical physics. © *2004 American Institute of Physics.*
[DOI: 10.1063/1.1635818]

I. INTRODUCTION

Highly spin-polarized sources for ions and electrons are of particular importance in chemical physics for the studies of spin-dependent scattering processes at a surface and in a gas phase, and characterizations of magnetic or semiconductor materials.[1–5] A standard spin-polarized electron source relies on photoemission from a GaAs crystal, which has been employed in spin-polarized electron microscopy, spin-polarized electron energy loss spectroscopy, and inverse photoelectron spectroscopy in materials science. The spin-polarized electron source utilized in high-energy accelerators can provide electrons with more than 80% polarization at currents as much as hundreds of microamperes. In contrast, for the studies of gas phase dynamics which are very important in chemical physics, energy-tunability, monochromaticity, and pulsed-operation are the desirable features for the spin-polarized electron source. To construct a spin-polarized source, an approach based on pulsed laser photoionization of atoms should be more favorable than the photoemission from a GaAs crystal, since the latter works only in an ultrahigh vacuum environment. Although not spin-polarized, monochromatic and low-energetic electrons produced by multiphoton ionization of atoms such as K and Ar by tunable pulsed lasers have been successfully applied to study the dissociative attachment.[6–8]

Spin polarization of atoms/ions by photoabsorption results from the transfer of angular momentum (helicity) of absorbed photons to the polarization of orbital angular momentum of electron, and finally to the spin angular momentum via spin–orbit interactions. There have been a lot of studies on photoionization in terms of the effect of the polarization and energy of photons on electron-spin polarization, among which it has been theoretically revealed that one-, two-, or three-photon ionization of alkali atoms can produce highly polarized photoelectrons, if a circularly polarized laser is tuned in the vicinity of fine-structure doublets.[9–11] Nakajima and Lambropoulos have theoretically investigated the productions of spin-polarized photoelectrons in one-, two-, and three-photon ionization of Xe, showing that the photoelectrons are nearly 100% polarized in the vicinity of autoionization states.[12] The use of noble gas such as Xe has greater advantages over alkali atoms in terms of the simplicity of increasing the number density, leading to the higher flux of spin-polarized electrons.

As for electron-spin-polarized ions, only a few studies based on optical pumping, spin-exchange, and multiphoton ionization techniques[13–16] have been reported, a more recent report being a fast Sr^+ beam source with an energy of several keV with more than 90% electron-spin polarization.[16]

If one is to utilize photoionization of atoms or molecules, highly spin-polarized photoelectrons and photoions may be simultaneously obtained. However, such an approach has not been recognized as a practical source of electron-spin-polarized charged particles, mainly due to the insufficient flux intensity of the particles produced in photoionization. In order to bring the flux intensity to the practical level, a method to increase the number density of precursor atoms

a)Electronic mail: nakajima@iae.kyoto-u.ac.jp

without breaking vacuum must be established. Moreover, realistic photoionization schemes which satisfy the necessary conditions of large cross sections and high electron-spin polarizations must be theoretically as well as experimentally investigated.

Recently, we have theoretically investigated two realistic schemes for the simultaneous production of electron-spin-polarized ions and spin-polarized electrons through photoionization from an excited triplet state; one-photon ionization from $5s5p\,^3P_1$ of Sr and one-photon near-resonant two-photon ionization via $5s5d\,^3D_{1,2}$ from $5s5p\,^3P_1$ of Sr.[17] The main findings are as follows: Electron-spin polarization of photoionized Sr^+ ions in the ground state $^2S_{1/2}$ can be more than 60%. A different choice of the laser polarization and the magnetic sublevel M_J of $5s5p\,^3P_1$ leads to the different degree of spin polarization. In addition, we have found that the degree of spin polarization of photoions and photoelectrons are exactly the same if all the produced photoions are in the ground $^2S_{1/2}$ state.

More recently, we have experimentally examined one of the two schemes mentioned above, i.e., one-photon ionization from the $5s5p\,^3P_1$ $(M_J=+1)$ state of Sr.[18] As having successfully applied to a source for atomic and molecular spectroscopy,[19–22] we produced Sr atoms by laser-ablation of a solid Sr disk. We have found that the Sr^+ $^2S_{1/2}$ ions produced through photoionization is highly electron-spin-polarized. Since laser-ablation can vaporize any metals and create a dense atomic gas without breaking vacuum, the combination of laser-ablation and photoionization by pulsed lasers would be a practical method to realize an intense pulsed source of electron-spin-polarized charge particles.

In the present paper, we report the detailed experimental results on electron-spin polarization of Sr^+ $^2S_{1/2}$ ions through one-photon ionization from the laser-excited $5s5p\,^3P_1$ $(M_J=+1)$ state of Sr atoms produced by laser-ablation. Complete experimental descriptions, including the characterization for the production of precursor Sr atoms by laser-ablation, will be given, which were not included in the previous paper.[18] Based on our previous theoretical work but with a more intuitive manner, we will explain why the spin-polarized photoions and photoelectrons are simultaneously produced.

II. EXPERIMENT

The level scheme we have employed to produce and probe the electron-spin polarization is illustrated in Fig. 1. Figure 2 shows the experimental geometry. A solid Sr disk mounted on a spinner was placed in a vacuum chamber which was evacuated to 1×10^{-4} Pa using a turbomolecular pump with a backup one. Vaporization of Sr was performed by focusing the ablation laser (Nd:YAG laser, Tempest, New Wave Research; 1064 nm, duration 10 ns, repetition rate 10 Hz, power density ~2 mJ/cm^2) onto the disk using an $f=250$ mm lens. An increase of the chamber pressure caused by laser-ablation was at most 1×10^{-4} Pa. Laser-ablated Sr atoms were excited to the $5s5p\,^3P_1$ $(M_J=+1)$ state by the pump laser beam (output of a pulsed dye laser FL3002, Lambda Physik; 689 nm, duration 15 ns, repetition rate 10 Hz, power density 110 μJ/50 mm^2), which was right-hand

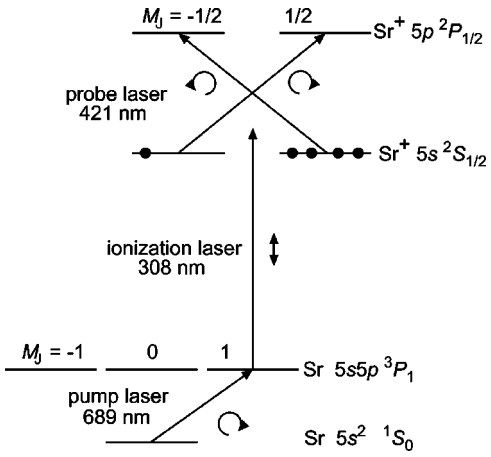

FIG. 1. Level scheme.

circularly polarized by a polarizing beamsplitter cube and a quarter wave plate. Then, atoms in $^3P_1$ were ionized by the ionization laser beam (output of a XeCl excimer laser, MSC103, Lambda Physik; 308 nm, duration 15 ns, repetition rate 10 Hz, power density 7 mJ/15 mm^2), which was linearly polarized by an UV polarizing beam splitter cube. Following photoionization, each of the $M_J=\pm1/2$ states of Sr^+ $5s\,^2S_{1/2}$ is alternately excited to the opposite-signed M_J state of $^2P_{1/2}$ using the probe laser beam (output of a pulsed dye laser FL3002 Lambda Physik; 421 nm, duration 15 ns, repetition rate 10 Hz, power density 50 nJ/50 mm^2), which is circularly polarized using similar optics to those of the pump laser beam; the left-hand and the right-hand circularly polarized (LHC/RHC) probe laser probes the populations in the $M_J=\pm1/2$ states of Sr^+ $5s\,^2S_{1/2}$, respectively (see Fig. 1). Those three lasers were spatially and temporally overlapped, and delayed by 50 μs from the ablation laser pulse using a digital pulse generator (DG535 Stanford Research). At the delay time of 50 μs, we have experimentally verified that the depolarization of electron-spin by the ablation itself was negligible, as described in the subsequent section. The pump and probe laser beams counterpropagated and crossed to the ionization laser at a right angle (see Fig. 2). In Fig. 1, we have chosen the quantization axis to be parallel to the propagation axis of the pump and probe lasers. Because of the experi-

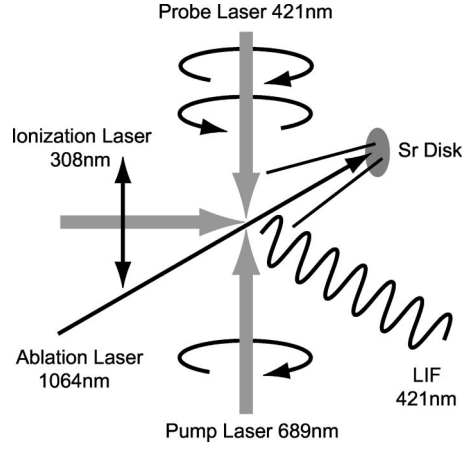

FIG. 2. Experimental geometry.

mental geometry (see Fig. 2), it is also parallel to the electric field vector of the ionization laser. The laser-induced fluorescence (LIF) signals from Sr^+ $^2P_{1/2}$ ($M_J=\pm 1/2$) to $^2S_{1/2}$ ($M_J=\mp 1/2$), which we call RHC-LIF and LHC-LIF, respectively, were alternately observed from the direction perpendicular to the quantization axis; they were collected and focused onto the slits of a monochromator (CT-25 JASCO) with a pair of lenses and detected by a photomutiplier tube (R955 Hamamatsu) which was temporally gated to avoid detecting intense continuum emission from the laser-ablation plume. The output from the photomutiplier tube was amplified and averaged using a fast preamplifier and a box-car integrator (Stanford Research). Since the spatial distributions of the LHC-LIF and RHC-LIF are identical and the detection sensitivity in the observation direction does not depend on the senses of polarization, no calibration for the LIF signals was conducted. Obviously, the intensities of the LHC-LIF and RHC-LIF signals should be directly proportional to $N_{\mathrm{ion}}^{\uparrow}$ and $N_{\mathrm{ion}}^{\downarrow}$, which are the populations in the Sr^+ $^2S_{1/2}$ ($M_J=\pm 1/2$) states, respectively. We define the experimental spin polarization of photoion, P_{ion}, to be

$$P_{\mathrm{ion}}=\frac{N_{\mathrm{ion}}^{\uparrow}-N_{\mathrm{ion}}^{\downarrow}}{N_{\mathrm{ion}}^{\uparrow}+N_{\mathrm{ion}}^{\downarrow}}=\frac{I_{\mathrm{LHC}}-I_{\mathrm{RHC}}}{I_{\mathrm{LHC}}+I_{\mathrm{RHC}}}, \tag{1}$$

where I_{LHC} and I_{RHC} are the intensities of the LHC-LIF and RHC-LIF signals, respectively.

The photoionization efficiency in the interaction region was estimated to be 10% for the pump laser intensity, 14 kW/cm^2, and the ionization one, 3.1 MW/cm^2.

III. RESULTS AND DISCUSSION

In this work Sr atoms were produced by laser-ablation of a solid Sr disk. Special care has to be taken to deduce the electron-spin polarization of Sr^+ $5s\,^2S_{1/2}$ ions from the LIF measurements, since the ablated species consist of not only neutral atoms in the $5s^2\,^1S_0$ ground state but also neutral atoms in the excited states as well as Sr^+ ions in various internal states. Therefore, the first thing we should check is that the contribution of undesired Sr^+ $5s\,^2S_{1/2}$ ions and Sr $5s5p\,^3P_{0,1,2}$ metastable atoms produced by laser-ablation itself on the electron-spin polarization measurement is negligible. The second one is that the depolarization of electron-spin by post-laser-ablation collisions is negligible. In the below we describe the procedures we have taken.

First, we examined how many particles in the interaction region remain in the Sr^+ $5s\,^2S_{1/2}$ state and the metastable Sr $5s5p\,^3P_{0,1,2}$ states after laser-ablation. Without the use of the pump and ionization lasers, we observed the LIF signal of $^2S_{1/2}$ Sr^+ ions. If the residual ions are electron spin-polarized, its contribution should be taken into account in the determination of electron-spin polarization produced by the present photoionization scheme. By the careful checking of the LIF signal, however, we confirmed that they were not electron-spin-polarized. Since the LIF signal was comparable with noise arising from the probe laser scattering, both of them are subtracted as a constant offset from the total signals when analyzing the LIF data. Next, we investigated the contribution of metastable $5s5p\,^3P_{0,1,2}$ Sr atoms to the electron-spin polarization measurement. If the non-negligible amount of atoms in the interaction region are in the metastable $5s5p\,^3P_{0,1,2}$ atoms after laser-ablation, they can be ionized by the 308 nm ionization laser only, resulting in the production of Sr^+ without the pump laser. This seriously prevents the reliable determination of electron-spin polarization from the LIF signal of Sr^+. In order to check if the non-negligible amount of atoms remain in the $5s5p\,^3P_{0,1,2}$ states after laser-ablation, we performed the LIF measurement without the pump laser. We have found no enhancement of the LIF signal, indicating that the contribution of $5s5p\,^3P_{0,1,2}$ atoms remaining in the interaction region by laser-ablation itself is negligible.

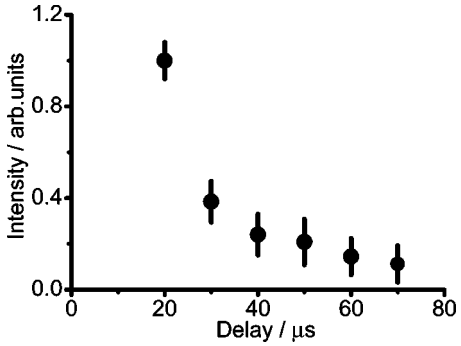

FIG. 3. Variation of the LIF signal of Sr^+, produced by photoionization of Sr, as a function of delay time after the ablation laser pulse.

Moreover, we examined the effects of post-laser-ablation collisions in terms of the depolarization of electron-spin of Sr^+ ions. Basically, a collision probability of particles depends on the number density. If the depolarization due to post-laser-ablation collisions takes place, electron-spin polarization should depend on the number density of Sr atoms as well. Figure 3 shows the temporal variation of the number density of $^1S_0$ Sr atoms in the interaction region after ablation, which was monitored as a trace of the LIF signal of Sr^+. No measurements at delay times shorter than 20 μs were conducted so as not to detect intense continuum emission from the ablation-plume. At delay times later than 80 μs, the LIF signal was too weak to detect. Obviously, the number density of the Sr atoms monotonically decreases as the delay time increases. Figure 4 shows the electron-spin polarization as a function of delay time after the ablation

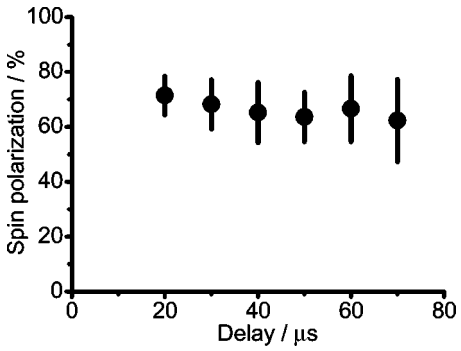

FIG. 4. Variation of the electron-spin polarization of Sr^+ as a function of delay time after the ablation laser pulse.

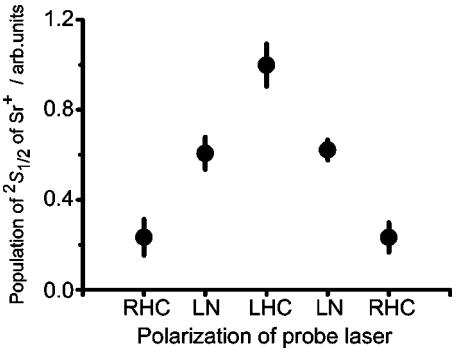

FIG. 5. LIF intensities of $^2S_{1/2}$ Sr^+ for different polarizations of the probe laser. RHC, LHC, and LN indicate right-/left-hand circular and linear polarizations of the probe laser, respectively.

pulse. In the entire range of delay time, electron-spin polarization is practically constant, and does not depend on the number density of Sr atoms. This means that the depolarization of electron-spin by post-laser-ablation collisions is negligible under our experimental conditions. Assuming that the Sr atoms travel with a constant velocity and knowing the 4 cm distance between the Sr disk and the interaction region, we could consider that the atoms appearing in the interaction region at the delay time of 20–70 μs have hyperthermal kinetic energies as much as 1 eV. Therefore, we could conclude that the thermal stagnation of the ablated particles in the interaction region does not occur. Rather, they pass away ballistically, satisfying a collision free condition.

In Fig. 5, we show the LIF intensity of the $^2S_{1/2}-^2P_{1/2}$ transition of Sr^+ produced by the photoionization from the $5s5p\,^3P_1$ state of Sr at the delay time of 50 μs, where the polarizations of the probing laser were set to be LHC, RHC and linear (LN). The plot profile is clearly symmetric, indicating that there is no phase deviation of the polarization configuration of the laser. Using data in Fig. 5 and Eq. (1), the experimental spin polarization of photoions, P_{ion}, is found to be $64\pm9\%$, where the error is statistical only.

The imperfectness of RHC polarization of the pump laser due to mixing of a LHC polarized component reduces the electron-spin polarization of photoions: The LHC polarized component produces the $^3P_1$ $M_J=-1$ states with the same ionization probability as the $^3P_1$ $M_J=+1$ states. Since the signs of the electron-spin polarizations of photoions produced from the $M_J=+1$ and -1 states are exactly opposite, the imperfectness of RHC polarization certainly reduces the electron-spin polarization of photoions. In the present case, sources of the imperfectness are undesirable phase retardations of the polarization optics and the window glass of the vacuum chamber. The former retardation is estimated to be 1 nm or less; the latter one is attributed to pressure-induced birefringence of the glass and estimated to be 2.1 nm from the photoelastic constant, the thickness of the glass and atmospheric pressure. According to our simple estimation, the LHC polarized component resulting from those retardations produces the $^3P_1$ $M_J=-1$ states of at most 1% and as a result the electron-spin polarization of photoions is reduced by 2% or less. Thus, the experimental spin polarization, P_{ion}, could be interpreted as having a systematic error of 2% or less due to the imperfectness of RHC polarization of the pump laser. If the power of the pump laser is strong enough to saturate the $^3P_1$ state, the reduction of the electron-spin polarization due to the imperfectness of RHC polarization will be serious. However, this is not our case, since we carefully checked the dependence of the photoion LIF intensity on the pump laser power and set the power level to $\sim25\%$ of the saturation level.

In our previous work,[17] we have theoretically studied the electron-spin polarizations of photoions and photoelectrons produced in the present photoionization scheme. In the calculations, a pure LS coupling with a single-term description of the relevant states and a single-electron transition approximation have been employed. Based on the calculation, the electron-spin polarization of photoions has been predicted to be in a range from 57% to 100%.[18] Obviously, the experimental electron-spin polarization of photoions is in the range.

If photoions are spin-polarized, it is expected that photoelectrons are also spin-polarized. However, the correspondence of the degrees of the spin polarizations between them is not *a priori* obvious and depends on the individual photoionization scheme and the atomic states involved in it. In the below, we make detailed analysis on the electron-spin polarizations of photoions and photoelectrons produced in the present photoionization scheme to evaluate the correspondence, which has not been performed in the previous theoretical work.[17]

In order to simplify the argument, we start with the description of the continuum in terms of the pure LS coupling. The effects of configuration mixing are introduced later on. Now, the parameters we need to specify the continuum are the wave vector, $\mathbf{k}$, of the photoelectron and the spin states, m_s and m_{Jc}, of the photoelectron and the residual ionic core which is necessarily in the Sr^+ $5s$ ($J_c=1/2$) state because of the wavelength of the ionization laser we have chosen. Note that the subscript c indicates that it is a quantum number associated with the core. In terms of the jj coupling, the continuum can be expanded using the partial waves, as

$$\begin{aligned}|\mathbf{k};m_s,m_{Jc}\rangle=&\sum_{l,m_l,j,J} a_{lm_l}|(J_cj)JM_J\rangle\\ &\times\langle(J_cj)JM_J|J_cm_{Jc}(ls)jm_j\rangle\\ &\times\langle(ls)jm_j|\mathbf{k};lm_lsm_s\rangle,\end{aligned}\tag{2}$$

where $a_{lm_l}=4\pi i^l e^{-i\delta_l}Y_{lm_l}(\Theta,\Phi)$ with (Θ,Φ) being the direction of outgoing photoelectrons. $\langle(J_cj)JM_J|J_cm_{Jc}(ls)jm_j\rangle$ and $\langle(ls)jm_j|\mathbf{k};lm_lsm_s\rangle$ are the Clebsch–Gordan coefficients and δ_l is the phase shift of the partial wave l. Using an LS-jj transformation matrix, $T_{LS,jj}$, given by

$$\begin{aligned}T_{LS,jj}=&\sqrt{(2L+1)(2S+1)(2J_c+1)(2j+1)}\\ &\times\begin{Bmatrix}L_c & l & L\\ S_c & s & S\\ J_c & j & J\end{Bmatrix},\end{aligned}\tag{3}$$

and recalling that the ionization takes from Sr $5s5p\,^3P_1$ ($M_J=+1$) which has a $5s5p\,^3P_1$ character with $\sim$99% purity,[17] the continuum of interest can be recast into the LS coupling form, as

$$\left|\mathbf{k};m_s=\frac{1}{2},m_{Jc}=\frac{1}{2}\right\rangle = a_{00}|5sks\,^3S_1M_J=1\rangle + a_{20}\left[\frac{1}{\sqrt{10}}|5skd\,^3D_1M_J=1\rangle - \frac{1}{\sqrt{2}}|5skd\,^3D_2M_J=1\rangle\right], \quad (4)$$

$$\left|\mathbf{k};m_s=\frac{1}{2},m_{Jc}=\frac{-1}{2}\right\rangle = a_{21}\left[-\frac{\sqrt{3}}{2\sqrt{5}}|5skd\,^3D_1M_J=1\rangle + \frac{\sqrt{3}}{6}|5skd\,^3D_2M_J=1\rangle - \frac{1}{\sqrt{2}}|5skd\,^1D_2M_J=1\rangle\right], \quad (5)$$

$$\left|\mathbf{k};m_s=\frac{-1}{2},m_{Jc}=\frac{1}{2}\right\rangle = a_{21}\left[-\frac{\sqrt{3}}{2\sqrt{5}}|5skd\,^3D_1M_J=1\rangle + \frac{\sqrt{3}}{6}|5skd\,^3D_2M_J=1\rangle + \frac{1}{\sqrt{2}}|5skd\,^1D_2M_J=1\rangle\right], \quad (6)$$

$$\left|\mathbf{k};m_s=\frac{-1}{2},m_{Jc}=\frac{-1}{2}\right\rangle = a_{22}\left[\sqrt{\frac{3}{5}}|5skd\,^3D_1M_J=1\rangle + \frac{1}{\sqrt{3}}|5skd\,^3D_2M_J=1\rangle\right]. \quad (7)$$

Therefore, the bound-free matrix elements $M[k,m_s,m_{Jc}]$ from $|5s5p\,^3P_1M_J=1\rangle$ into all the accessible continua with the spin states labeled by m_s and m_{Jc} for the photoelectron and the photoion are

$$M\left[k,m_s=\frac{1}{2},m_{Jc}=\frac{1}{2}\right] = a_{00}\langle 5sks\,^3S_1M_J=1|r_0|5s5p\,^3P_1M_J=1\rangle + a_{20}\left[\frac{1}{\sqrt{10}}\langle 5skd\,^3D_1M_J=1|r_0|5s5p\,^3P_1M_J=1\rangle - \frac{1}{\sqrt{2}}\langle 5skd\,^3D_2M_J=1|r_0|5s5p\,^3P_1M_J=1\rangle\right], \quad (8)$$

$$M\left[k,m_s=\frac{1}{2},m_{Jc}=\frac{-1}{2}\right] = a_{21}\left[-\frac{\sqrt{3}}{2\sqrt{5}}\langle 5skd\,^3D_1M_J=1|r_0|5s5p\,^3P_1M_J=1\rangle + \frac{\sqrt{3}}{6}\langle 5skd\,^3D_2M_J=1|r_0|5s5p\,^3P_1M_J=1\rangle - \frac{1}{\sqrt{2}}\langle 5skd\,^1D_2M_J=1|r_0|5s5p\,^3P_1M_J=1\rangle\right], \quad (9)$$

$$M\left[k,m_s=\frac{-1}{2},m_{Jc}=\frac{1}{2}\right] = a_{21}\left[-\frac{\sqrt{3}}{2\sqrt{5}}\langle 5skd\,^3D_1M_J=1|r_0|5s5p\,^3P_1M_J=1\rangle + \frac{\sqrt{3}}{6}\langle 5skd\,^3D_2M_J=1|r_0|5s5p\,^3P_1M_J=1\rangle + \frac{1}{\sqrt{2}}\langle 5skd\,^1D_2M_J=1|r_0|5s5p\,^3P_1M_J=1\rangle\right], \quad (10)$$

$$M\left[k,m_s=\frac{-1}{2},m_{Jc}=\frac{-1}{2}\right]=0. \quad (11)$$

Using these quantities defined above, the photoion yields with spin up and down are

$$Q_{\mathrm{ion}}^{\uparrow} = \sum_{m_s=\pm 1/2}\int d\Omega\left|M\left[k,m_s,m_{Jc}=\frac{1}{2}\right]\right|^2, \quad (12)$$

$$Q_{\mathrm{ion}}^{\downarrow} = \sum_{m_s=\pm 1/2}\int d\Omega\left|M\left[k,m_s,m_{Jc}=\frac{-1}{2}\right]\right|^2. \quad (13)$$

Similarly, the photoelectron yields with spin up and down are

$$Q_{\mathrm{ele}}^{\uparrow} = \sum_{m_{Jc}=\pm 1/2}\int d\Omega\left|M\left[k,m_s=\frac{1}{2},m_{Jc}\right]\right|^2, \quad (14)$$

$$Q_{\mathrm{ele}}^{\downarrow} = \sum_{m_{Jc}=\pm 1/2}\int d\Omega\left|M\left[k,m_s=\frac{-1}{2},m_{Jc}\right]\right|^2. \quad (15)$$

Electron-spin polarization of photoions and photoelectrons are obtained as

$$P_{\mathrm{ion}}=\frac{Q_{\mathrm{ion}}^{\uparrow}-Q_{\mathrm{ion}}^{\downarrow}}{Q_{\mathrm{ion}}^{\uparrow}+Q_{\mathrm{ion}}^{\downarrow}}, \tag{16}$$

$$P_{\mathrm{ele}}=\frac{Q_{\mathrm{ele}}^{\uparrow}-Q_{\mathrm{ele}}^{\downarrow}}{Q_{\mathrm{ele}}^{\uparrow}+Q_{\mathrm{ele}}^{\downarrow}}. \tag{17}$$

As long as the LS coupling is a good approximation to describe the continuum as we have assumed so far, a certain conclusion can be deduced without knowing the exact values of matrix elements in the above expressions. We note that spin–orbit interactions in the continuum exist even under the LS coupling condition. The effects of spin–orbit interaction in the continuum can be reflected by the different values of bound-free matrix elements for $\langle 5skd\,^3D_1M_J=1|r_0|5s5p\,^3P_1M_J=1\rangle$ and $\langle 5skd\,^3D_2M_J=1|r_0|5s5p\,^3P_1M_J=1\rangle$. From the above expressions, we find that, as long as the singlet–triplet transition is negligible upon ionization, i.e., under the good LS coupling condition, the last terms in Eqs. (9) and (10) may be neglected. Therefore we arrive at $P_{\mathrm{ele}}\approx P_{\mathrm{ion}}$ *as long as the system under consideration is well described by the LS coupling*. Similarly, if the initial state is a pure singlet state such as $5s5p\,^1P_1$ $M_J=1$ instead of $5s5p\,^3P_1$ $M_J=1$, then, it is straightforward to obtain $P_{\mathrm{ele}}\approx P_{\mathrm{ion}}=0$ which we have already found in Ref. 17. As a last remark under the good LS coupling condition, we note that, if we further introduce the single-electron transition approximation, $P_{\mathrm{ion}}(\approx P_{\mathrm{ele}})$ can be reduced to Eq. (2) in Ref. 18.

Now, we proceed further to introduce configuration mixing between the continua of interest. The simplest way to introduce configuration mixing is to replace $|5sks\,^3S_1M_J=1\rangle$ and $|5skd\,^3D_1M_J=1\rangle$, and also $|5sks\,^3D_2M_J=1\rangle$ and $|5skd\,^1D_2M_J=1\rangle$ in Eqs. (8)–(11) by $\cos\alpha|5sks\,^3S_1M_J=1\rangle - \sin\alpha|5skd\,^3D_1M_J=1\rangle$ and $\sin\alpha|5sks\,^3S_1M_J=1\rangle + \cos\alpha|5skd\,^3D_1M_J=1\rangle$, and $\cos\beta|5sks\,^3D_2M_J=1\rangle - \sin\beta|5skd\,^1D_2M_J=1\rangle$ and $\sin\beta|5sks\,^3D_2M_J=1\rangle + \cos\beta|5skd\,^1D_2M_J=1\rangle$, where α and β are the mixing angles. However, since we are not able to calculate the configuration mixing for the continua, we calculate, instead, the configuration mixing for the bound Rydberg states of $5snd\,^1D_2$ and $5snd\,^3D_2$ around $n\sim 10$ using a Hartree–Fock code.[25] $4d6s$ configuration is also included for the calculations, for it is known to perturb $5snd$ states. We have found that $5sns\,^3S_1$ ($n\sim 10$) contains no more than a few % of the $5snd\,^3D_1$ and $4d6s\,^3D_1$ character, and $5snd\,^3D_1$ ($n\sim 10$) contains no more than a few % of the $5sns\,^3S_1$ and $4d6s\,^3D_1$ characters. We have also found that $5snd\,^3D_2$ ($n\sim 10$) contains no more than a few % of the $5snd\,^1D_2$ and $4d6s\,^1D_2$ characters and vice versa. Similar tendency can be expected for the continua lying near the ionization threshold. After these considerations, we infer that, although we did not directly measure the degree of spin polarization of photoelectrons, its value would be within a few % accuracy from that of photoions which we did measure. For more quantitative comparison, of course, it is necessary to carry out direct measurements of spin polarization of photoelectrons and compare with that of photoions.

So far we did not take into account the depolarization of electron-spin due to hyperfine interactions (hyperfine depolarization). The hyperfine depolarization is relevant only to ^{87}Sr with nuclear spin $I=9/2$. Hyperfine structure of the neutral $5s5p\,^3P_1$ state could cause depolarization *upon production* of electron-spin-polarized ions, while that of the ionic Sr^+ $5s\,^2S_{1/2}$ and $5p\,^2P_{1/2}$ states could cause apparent depolarization *upon measurement*. Note that the effective hyperfine coupling time is given by the inverse of hyperfine splitting. Briefly, the hyperfine interaction transfers a part of population in some M_J state to the other M_J state. As for the produced Sr^+ ion, the hyperfine energy splittings of both $^2S_{1/2}$ and $^2P_{1/2}$ states[23,24] are smaller than the probe laser bandwidth and the inverse of the spontaneous decay time of the upper $^2P_{1/2}$ state. Therefore, the hyperfine interaction of Sr^+ ions upon electron-spin polarization measurement can be safely neglected. Regarding the neutral Sr atom, depolarization arising from the reduction of state selectivity does also exist due to the nuclear spin ($I=9/2$) for ^{87}Sr: Even with $I=9/2$, the magnetic quantum number of the ground state $5s^2\,^1S_0$ can take only one value of $M_J=0$. On the other hand, the upper $5s5p\,^3P_1$ state splits into three hyperfine levels, each of which consists of several magnetic sublevels. Since our pump laser does not resolve the hyperfine structure of $5s5p\,^3P_1$, the laser-excited $5s5p\,^3P_1$ state becomes a superposition of all M_J's with different amplitudes. This is nothing but the reduction of state selectivity into particular M_J, leading to depolarization. Since the natural abundance of ^{87}Sr is 7%, electron-spin polarization obtained in the present measurement should be regarded as having an uncertainty of at most 7% due to the reduction of state selectivity.

IV. CONCLUSION

In conclusion, we have carried out the detailed study on the production of electron-spin-polarized Sr^+ ions. Laser-ablation has been employed for the production of Sr atoms prior to photoionization. We have experimentally confirmed that the laser-ablation does not affect the electron-spin polarization in terms of the production and the measurement. $64\pm 9\%$ electron-spin polarization of $5s\,^2S_{1/2}$ Sr^+ ions has been found through one-photon ionization from the laser-excited $5s5p\,^3P_1$ ($M_J=+1$) state of Sr produced by laser-ablation. The experimentally determined electron-spin polarization of Sr^+ ions is in good agreement with the previous theoretical prediction, which also ensures that the photoelectrons, being the counterpart of Sr^+ ions upon photoionization, have approximately the same degree of spin polarization as long as the LS-coupling description is valid. We have also given an explanation of why the electron-spin polarization of ions and electrons are *approximately* the same for our particular case. In order to verify our analysis, however, it is necessary to measure the spin polarization of both photoions and photoelectrons and compare them. Our experimental results demonstrate that the combination of laser-ablation and photoionization by pulsed lasers would be an effective method to realize an intense pulsed source of spin-polarized ions.

ACKNOWLEDGMENT

This work was supported by the Grant-in-Aid for scientific research from the Ministry of Education and Science of Japan.

[1] J. Kessler, *Polarized Electrons*, 2nd ed. (Springer-Verlag, Berlin, 1985).
[2] U. Heinzmann and N. A. Cherepkov, *VUV and Soft-X-Ray Photoionization*, edited by U. Becker and D. A. Shirley (Plenum, New York, 1996), p. 521.
[3] A. V. Subashiev, Phys. Low-Dimens. Semicond. Struct. **1–2**, 1 (1999).
[4] J. E. Clendenin, Int. J. Mod. Phys. A **13**, 2507 (1998).
[5] A. V. Subashiev and J. E. Clendennin, Int. J. Mod. Phys. A **15**, 2519 (2000).
[6] J. M. Weber, E. Leber, M.-W. Ruf, and H. Hotop, Phys. Rev. Lett. **82**, 516 (1999).
[7] A. Schramm, J. M. Weber, J. Kreil, D. Klar, M.-W. Ruf, and H. Hotop, Phys. Rev. Lett. **81**, 778 (1998).
[8] P.-T. Howe, A. Kortyna, M. Darrach, and A. Chutjian, Phys. Rev. A **64**, 042706 (2001).
[9] P. Lambropoulos, Phys. Rev. Lett. **30**, 413 (1973).
[10] S. N. Dixit, P. Lambropoulos, and P. Zoller, Phys. Rev. A **24**, 318 (1981).
[11] E. Sokell, S. Zamith, M. A. Bouchene, and B. Girard, J. Phys. B **33**, 2005 (2000).
[12] T. Nakajima and P. Lambropoulos, Europhys. Lett. **57**, 25 (2002).
[13] J. Ganz, B. Lewandowski, A. Siegel, W. Bussert, H. Waibel, M.-W. Ruf, and H. Hotop, J. Phys. B **15**, 1485 (1982).
[14] D. L. Bixler, J. C. Lancaster, F. J. Kontur, R. A. Popple, F. B. Dunning, and G. K. Walters, Rev. Sci. Instrum. **70**, 240 (1999).
[15] L. W. Anderson, Nucl. Instrum. Methods Phys. Res. A **402**, 179 (1998).
[16] H. Reihl, C. Sprengel, Z. Roller-Lutz, and H. O. Lutz, Nucl. Instrum. Methods Phys. Res. A **357**, 225 (1995).
[17] T. Nakajima and N. Yonekura, J. Chem. Phys. **117**, 2112 (2002).
[18] T. Nakajima, N. Yonekura, Y. Matsuo, T. Kobayashi, and Y. Fukuyama, Appl. Phys. Lett. **83**, 2103 (2003).
[19] T. Nakajima, Y. Matsuo, N. Yonekura, M. Nakamura, and M. Takami, J. Phys. B **31**, 1729 (1997).
[20] N. Yonekura, T. Nakajima, Q. Hui, and M. Takami, Chem. Phys. Lett. **280**, 525 (1997).
[21] T. Nakajima, N. Yonekura, Y. Matsuo, Q. Hui, and M. Takami, Phys. Rev. A **57**, 3598 (1998).
[22] Y. Matsuo, T. Nakajima, T. Kobayashi, and M. Takami, Appl. Phys. Lett. **71**, 996 (1997).
[23] G. Borghs, P. De Bisschop, M. Van Hove, and R. E. Silverans, Hyperfine Interact. **16**, 177 (1983).
[24] H. Sunaoshi, Y. Fukashiro, M. Furukawa, M. Yamauchi, S. Hayashibe, T. Shinozuka, M. Fujioka, I. Satoh, M. Wada, and S. Matsuki, Hyperfine Interact. **78**, 241 (1993).
[25] R. D. Cowan, *The Theory of Atomic Structure and Spectra* (University of California Press, Berkeley, 1981).